JCI insight

Tissue-resident macrophages can contain replication-competent virus in antiretroviral-naive, SIV-infected Asian macaques

Sarah R. DiNapoli, … , Kenneth Knox, Jason M. Brenchley

JCI Insight. 2017;2(4):e91214. https://doi.org/10.1172/jci.insight.91214.

Research Article AIDS/HIV

SIV DNA can be detected in lymphoid tissue–resident macrophages of chronically SIV-infected Asian macaques. These macrophages also contain evidence of recently phagocytosed SIV-infected $CD4^+$ T cells. Here, we examine whether these macrophages contain replication-competent virus, whether viral DNA can be detected in tissue-resident macrophages from antiretroviral (ARV) therapy–treated animals and humans, and how the viral sequences amplified from macrophages and contemporaneous $CD4^+$ T cells compare. In ARV-naive animals, we find that lymphoid tissue–resident macrophages contain replication-competent virus if they also contain viral DNA in ARV-naive Asian macaques. The genetic sequence of the virus within these macrophages is similar to those within $CD4^+$ T cells from the same anatomic sites. In ARV-treated animals, we find that viral DNA can be amplified from lymphoid tissue–resident macrophages of SIV-infected Asian macaques that were treated with ARVs for at least 5 months, but we could not detect replication-competent virus from macrophages of animals treated with ARVs. Finally, we could not detect viral DNA in alveolar macrophages from HIV-infected individuals who received ARVs for 3 years and had undetectable viral loads. These data demonstrate that macrophages can contain replication-competent virus, but may not represent a significant reservoir for HIV in vivo.

JCI insight

RESEARCH ARTICLE

Tissue-resident macrophages can contain replication-competent virus in antiretroviral-naive, SIV-infected Asian macaques

Sarah R. DiNapoli,[1] Alexandra M. Ortiz,[1] Fan Wu,[2] Kenta Matsuda,[2] Homer L. Twigg III,[3] Vanessa M. Hirsch,[2] Kenneth Knox,[4] and Jason M. Brenchley[1]

[1]Laboratory of Parasitic Diseases, [2]Laboratory of Molecular Microbiology, National Institute of Allergy and Infectious Diseases, NIH, Bethesda, Maryland, USA. [3]Department of Medicine, Indiana University, Indianapolis, Indiana, USA. [4]Department of Medicine, University of Arizona, Tucson, Arizona, USA.

SIV DNA can be detected in lymphoid tissue–resident macrophages of chronically SIV-infected Asian macaques. These macrophages also contain evidence of recently phagocytosed SIV-infected CD4$^+$ T cells. Here, we examine whether these macrophages contain replication-competent virus, whether viral DNA can be detected in tissue-resident macrophages from antiretroviral (ARV) therapy–treated animals and humans, and how the viral sequences amplified from macrophages and contemporaneous CD4$^+$ T cells compare. In ARV-naive animals, we find that lymphoid tissue–resident macrophages contain replication-competent virus if they also contain viral DNA in ARV-naive Asian macaques. The genetic sequence of the virus within these macrophages is similar to those within CD4$^+$ T cells from the same anatomic sites. In ARV-treated animals, we find that viral DNA can be amplified from lymphoid tissue–resident macrophages of SIV-infected Asian macaques that were treated with ARVs for at least 5 months, but we could not detect replication-competent virus from macrophages of animals treated with ARVs. Finally, we could not detect viral DNA in alveolar macrophages from HIV-infected individuals who received ARVs for 3 years and had undetectable viral loads. These data demonstrate that macrophages can contain replication-competent virus, but may not represent a significant reservoir for HIV in vivo.

Introduction

HIV remains a major global health burden despite advances in antiretroviral (ARV) therapy. Although current ARV therapy can effectively suppress viral activity and reduce plasma viral load to undetectable levels, treatment must be maintained for the lifetime of HIV-infected individuals to prevent viral rebound from the latent viral reservoir (1–4). Characterizing the reservoir of latently infected cells — cell type, anatomic location, and longevity — is critical for developing strategies to eradicate the virus. While CD4$^+$ T cells are the predominant target for HIV and SIV in vivo, myeloid cells have also been identified as targets for HIV/SIV. Macrophages are of interest as potential sources of latent virus because of their reported longevity in tissues after differentiation (although recent data have shown that macrophages may proliferate homeostatically) (5–8).

In the CNS, macrophages (microglial cells and perivascular macrophages) have been reported to support viral replication in vivo (9–19). HIV infection of brain-resident macrophages has been associated with development of HIV-1–associated dementia (HAD), encephalitis, and other neurocognitive disorders in HIV-infected individuals (15). Numerous studies have reported in vitro macrophage infection with virus isolated from brain tissues and/or cerebrospinal fluid of HIV-infected individuals and Asian macaques infected with a neurotropic strain of SIV (20–26). Determining how HIV/SIV reaches the brain, whether it establishes a reservoir of replication-competent virus, and how highly active antiretroviral therapy (HAART) impacts HIV/SIV in the CNS remains an open area of investigation. Recent studies have detected HIV/SIV in parenchymal microglia (17, 18), ARV-naive patients' cerebrospinal fluid (26), and proliferating perivascular macrophages (8). Interestingly, although these studies detect HIV/SIV in the CNS, they

Conflict of interest: The authors have declared that no conflict of interest exists.

Submitted: October 14, 2016
Accepted: January 5, 2017
Published: February 23, 2017

Reference information:
JCI Insight. 2017;2(4):e91214. https://doi.org/10.1172/jci.insight.91214.

offer differing perspectives on whether HIV is actively replicating in the CNS and on microglial cell longevity and origin. Further investigation of microglial cell and perivascular macrophage dynamics and infection in the CNS is needed. With the advent of HAART, the incidence and severity of HAD has decreased; however, HIV infection in the CNS remains of interest for characterizing the latent viral reservoir, particularly given lower penetrance of ARVs across the blood-brain barrier (27–30). Outside of the CNS, viral DNA has been detected in alveolar macrophages from bronchoalveolar lavage (BAL) (31–33) and in $CD3^-$ cells presumed to be macrophages in the gastrointestinal tract (32, 34).

Given the limitations in sampling tissues from HIV-infected individuals, animal models of HIV infection offer valuable opportunities to investigate viral infection and latency longitudinally and across tissue types. Indeed, several SIV models have reported evidence of viral replication in macrophages in vivo (8, 17, 35–41). These studies generally identified macrophage infection by detection of viral nucleic acids by in situ hybridization or immunohistochemistry. However, these methods do not necessarily indicate the presence of replication-competent virus, as the pool of nonfunctional viral DNA and RNA vastly exceeds the pool of coding viral proviruses (42). Further, models where SIV has been shown to replicate in macrophages in vivo have 2 main characteristics in common: rapid disease progression and massive $CD4^+$ depletion — both patterns are rarely observed in canonical HIV/SIV infection (40). While these SIV models demonstrate the capacity for viral replication in macrophages, additional work examining the role of macrophages in conventional HIV/SIV infections, macrophage infection in the context of ARV therapy, and determining whether macrophages harbor replication-competent virus and in what tissues is necessary.

Recently, we surveyed $CD4^+$ T cell subsets and myeloid cells isolated from mucosal and lymphoid tissues for viral DNA levels in a large cohort of SIV-infected Asian macaques (43). While only 2 animals had viral DNA^+ myeloid cells from mucosal tissues, we amplified viral DNA from lymphoid tissue–resident myeloid cells in 40% of the animals surveyed. That we primarily detected viral DNA in lymphoid myeloid cells suggested that myeloid cells contain viral DNA in tissues where $CD4^+$ T cells persist (compared with mucosal sites where $CD4^+$ T cells are massively depleted throughout infection). We then performed quantitative PCR for rearranged TCR-γδ DNA in myeloid cells and concluded that macrophages can acquire viral DNA via phagocytosis of SIV-infected $CD4^+$ T cells from the surrounding tissue. Detecting viral DNA in tissue macrophages indicates the potential for productive infection of macrophages. Indeed, recent in vitro data demonstrated that macrophages can become infected with HIV via phagocytosis of infected $CD4^+$ T cells (44). However, our previous analysis for viral DNA alone did not determine whether or not lymphoid tissue–resident myeloid cells contain replication-competent virus in vivo.

Here, we have examined myeloid cells from the lymphoid tissues of SIV-infected Asian macaques to determine (a) if viral DNA^+ macrophages contain replication-competent virus; (b) how sequences of virus isolated from contemporaneous $CD4^+$ T cells and macrophages compare; (c) whether viral DNA and replication-competent virus can be detected in lymphoid tissue–resident macrophages from ARV-treated animals; and (d) whether tissue-resident macrophages from ARV-treated, HIV-infected individuals have evidence of HIV infection. We found that macrophages with detectable viral DNA can contain replication-competent virus in ARV-naive animals, that the viruses from $CD4^+$ T cells and macrophages are genetically similar, that we were not able to rescue replication-competent virus from lymphoid tissue–resident macrophages from ARV-treated animals despite detection of viral DNA^+ macrophages, and that alveolar macrophages from ARV-treated, HIV-infected individuals with undetectable plasma viremia contained undetectable levels of HIV DNA.

Results

Study design. To investigate whether myeloid cells harbor replication-competent virus in vivo and in the context of ARV therapy, we isolated tissue-resident macrophages from lymphoid tissues taken at necropsy of SIV-infected Asian macaques (Table 1). These animals were infected with either SIVsmE543 or SIVmac239 and were sacrificed at various disease stages ranging from the acute phase to simian AIDS (26 animals). These animals had a range of $CD4^+$ T cell counts and viral loads reflecting different disease states. The variety of SIV inocula and disease states offers a range of conditions to assess cellular targeting.

To determine whether viral DNA and replication-competent virus can be detected in lymphoid tissue–resident myeloid cells after ARV therapy, we isolated leukocytes from splenic tissue taken at necropsy from a cohort of 19 chronically SIVmac239-infected pigtail macaques that received ARV therapy for at least 5 months (Table 1). These animals had a range of $CD4^+$ T cell counts and had undetectable plasma viral loads in all but 2 animals.

Table 1. Study animal characteristics

Animal	Virus	Species	CD4+ T cells[A]	Viral load[B]	ARV Duration[C]	Disease state
Rh591	E543	RM	186	2.5×10^5	NA	Chronic
Rh760	E543	RM	296	5.0×10^3	NA	Chronic
Rh759	E543	RM	526	6.0×10^2	NA	Chronic
Rh827	E543	RM	69	3.7×10^5	NA	sAIDS
Rh833	E543	RM	133	1.5×10^5	NA	sAIDS
Rh848	E543	RM	182	2.2×10^6	NA	sAIDS
RhDB07	mac239	RM	317	5.5×10^5	NA	Chronic
RhDB92	mac239	RM	194	1.0×10^5	NA	Chronic
RhDB4E	mac239	RM	565	8.1×10^5	NA	Chronic
RhDCXX	mac239	RM	439	1.5×10^6	NA	Chronic
RhCF5T	mac239	RM	216	8.0×10^5	NA	sAIDS
RhDB17	mac239	RM	122	9.2×10^4	NA	sAIDS
RhPSP	mac239	RM	194	7.8×10^6	NA	sAIDS
RhCF4J	mac239	RM	241	2.0×10^5	NA	sAIDS
RhCE5D	mac239	RM	532	1.2×10^5	NA	sAIDS
RhA8E084	mac239	RM	513	1.1×10^6	NA	Acute
RhK7M	mac239	RM	188	2.4×10^6	NA	Acute
RhK8Y	mac239	RM	1855	8.4×10^7	NA	Acute
99P029	mac239	PTM	8	5.4×10^6	NA	Chronic
A1P012	mac239	PTM	5	4.2×10^5	NA	Chronic
98P030	mac239	PTM	178	7.2×10^3	NA	Chronic
99P030	mac239	PTM	29	3.7×10^4	NA	sAIDS
A0P007	mac239	PTM	30	4.9×10^4	NA	sAIDS
98P005	mac239	PTM	33	7.6×10^3	NA	sAIDS
A0P039	mac239	PTM	45	1.9×10^4	NA	sAIDS
99P052	mac239	PTM	30	6.4×10^5	NA	sAIDS
PTA2P028	mac239	PTM	230	Undetected	266	NA
PT11263	mac239	PTM	771	Undetected	268	NA
PT11264	mac239	PTM	766	Undetected	263	NA
PTA2P033	mac239	PTM	232	340	24	NA
PTA2P036	mac239	PTM	221	Undetected	275	NA
PTGB21	mac239	PTM	203	Undetected	263	NA
PTGE04	mac239	PTM	421	Undetected	260	NA
PTA0P031	mac239	PTM	362	Undetected	267	NA
PTA2P011	mac239	PTM	143	Undetected	267	NA
PTA2P031	mac239	PTM	385	92	266	NA
PTGE34	mac239	PTM	337	Undetected	150	NA
PTA2P032	mac239	PTM	438	Undetected	150	NA
PTA11266	mac239	PTM	943	Undetected	267	NA
PTGP27	mac239	PTM	892	Undetected	150	NA
PTGE36	mac239	PTM	100	Undetected	150	NA
PTGE40	mac239	PTM	682	Undetected	150	NA
PTGD97	mac239	PTM	619	Undetected	150	NA
PTFR60	mac239	PTM	511	Undetected	150	NA
PTGC45	mac239	PTM	305	Undetected	150	NA

[A]Number of CD4+ T cells/μl blood. [B]Copies viral RNA/ml of plasma. [C]Antiretroviral (ARV) duration in days. RM, rhesus macaque; PTM, pigtailed macaque, sAIDS, simian AIDS.

Replication-competent virus in lymphoid tissue–resident macrophages. Previously, we detected viral DNA in lymphoid tissue–resident myeloid cells of approximately 40% of ARV-naive, SIV-infected animals (43). To determine whether the detected viral DNA represents replication-competent virus in lymphoid tissue–resident myeloid cells, we flow cytometrically sorted memory CD4+ T cells and myeloid cells from the spleen or mesenteric lymph node of 7 ARV-naive, SIV-infected Asian macaques with viral DNA+ lymphoid myeloid cells (Supplemental Figure 1; supplemental material available online with

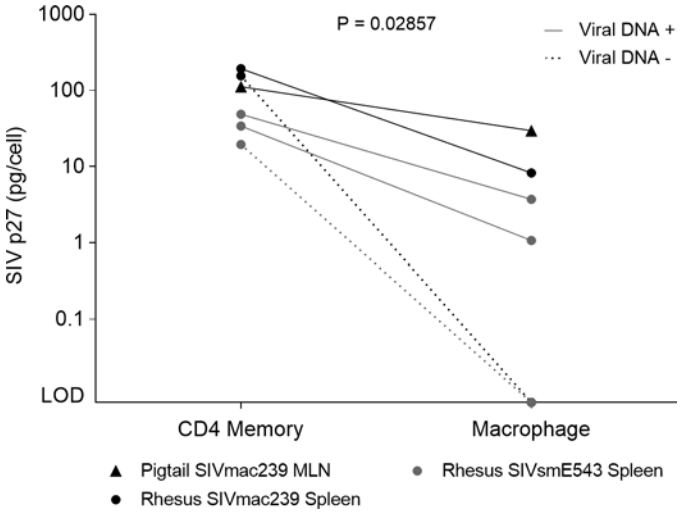

Figure 1. Replication-competent virus in ARV-naive lymphoid tissues. SIV p27 levels in cell culture media from cocultures of memory CD4$^+$ T cells (left) or myeloid cells (right) with CEMx174 cells after 1 week. Cells were sorted from the spleen or mesenteric lymph node (MLN). SIV p27 levels in memory CD4$^+$ T cell cocultures and macrophage cocultures (excluding viral DNA$^-$ animals) were compared via Mann-Whitney test (P = 0.02857). Reported values are pg SIV p27 per primary cell added to the coculture (8×10^3 sorted cells and 5×10^4 CEMx174 cells per well). LOD, limit of detection.

this article; https://doi.org/10.1172/jci.insight.91214DS1). The sorted cells were then cocultured with CEMx174 cells for 3 weeks and cell culture media samples were collected for analysis of virus production via ELISA for SIV p27 Gag (Figure 1). The CEMx174 cell line is highly permissive to infection with sooty mangabey–lineage SIV strains and efficiently amplifies low levels of replication-competent virus (45). This technique is more sensitive in amplifying low levels of virus than cocultures with allogenic primary cells. Irrespective of SIV virus type, we find that CEMx174 cells support viral replication better than either monocyte-derived macrophages or primary CD4$^+$ T cells (Hirsch, unpublished observations). Although differing replication kinetics could impact detection of replication-competent virus, we maintained cell cultures for 3 weeks and were able to detect viral replication from animals with a range of macrophage viral DNA levels. For each animal, we detected viral replication in the cell culture media from coculture with memory CD4$^+$ T cells. In 4 animals, we also detected viral replication in cell culture media from coculture with myeloid cells. The levels of SIV p27 detected in culture media after 1 week were lower from myeloid cell cocultures compared with memory CD4$^+$ T cell cocultures (P = 0.029). Two animals previously reported to have no viral DNA in lymphoid myeloid cells were also analyzed by coculture (Rh760 and RhDB07) and had no detectable SIV in the myeloid cell coculture media.

Genetic comparison of replication-competent virus from memory CD4$^+$ T cells and myeloid cells. Characterization of HIV/SIV infection of macrophages — including genetic determinants of macrophage tropism and potential viral evolution towards infection of macrophages over the course of infection — remains an open area of investigation. As shown in Figure 1, we detected replication-competent virus in memory CD4$^+$ T cells and myeloid cells in animals with previously reported detectable viral DNA. To investigate whether the viruses generated in coculture of CEMx174 cells with myeloid cells are genetically comparable to viruses from coculture with memory CD4$^+$ T cells, or whether the viruses within these macrophages had significantly evolved from the viruses within CD4$^+$ T cells, we extracted viral RNA from cell culture media and compared sequences of variable regions 1–4 (V1–V4) of SIV envelope (*Env*) protein. In addition, viral RNA was extracted from contemporaneous plasma samples for each animal to determine whether viral sequences from tissue-resident cells were compartmentalized compared to circulating virus in the plasma.

Phylogenies of the *Env* sequences for each animal were constructed using the Kimura 2-parameter model and analyzed for strength of branch support by bootstrapping (Figure 2). Of the 4 animals with replication-competent virus in myeloid cells, *Env* sequences from myeloid cell cocultures were distributed across the phylogeny for 1 animal (99P052, Figure 2A) and clustered together for 3 animals (Figure 2, B–D). CD4$^+$ T cell coculture and contemporaneous plasma *Env* sequences were distributed throughout each tree in 3 of the 4 animals, with some clustering from each compartment in Rh848 (Figure 2C). Two of the 4 animals had simian AIDS at necropsy (Rh848 and 99P052). Irrespective of disease state, the phylogenies of both animals did not indicate significant divergence of *Env* sequences associated with macrophages and memory CD4$^+$ T cells.

Bootstrap analysis of each tree indicated limited significance of branching at most nodes in each tree. Few nodes had bootstrap values over 70 — a common threshold for significant branching — suggesting that genetic differences in each sequence were minor and insufficient for strong phylogenetic distinction. Of the 4 phylogenies, Rh591 had the greatest apparent compartmentalization of macrophage sequences. Posterior probability analysis indicated that there is an 83% chance that macrophage-associated *Env* sequences were indeed different from CD4$^+$ T cell–associated sequences from Rh591 (Figure 2D).

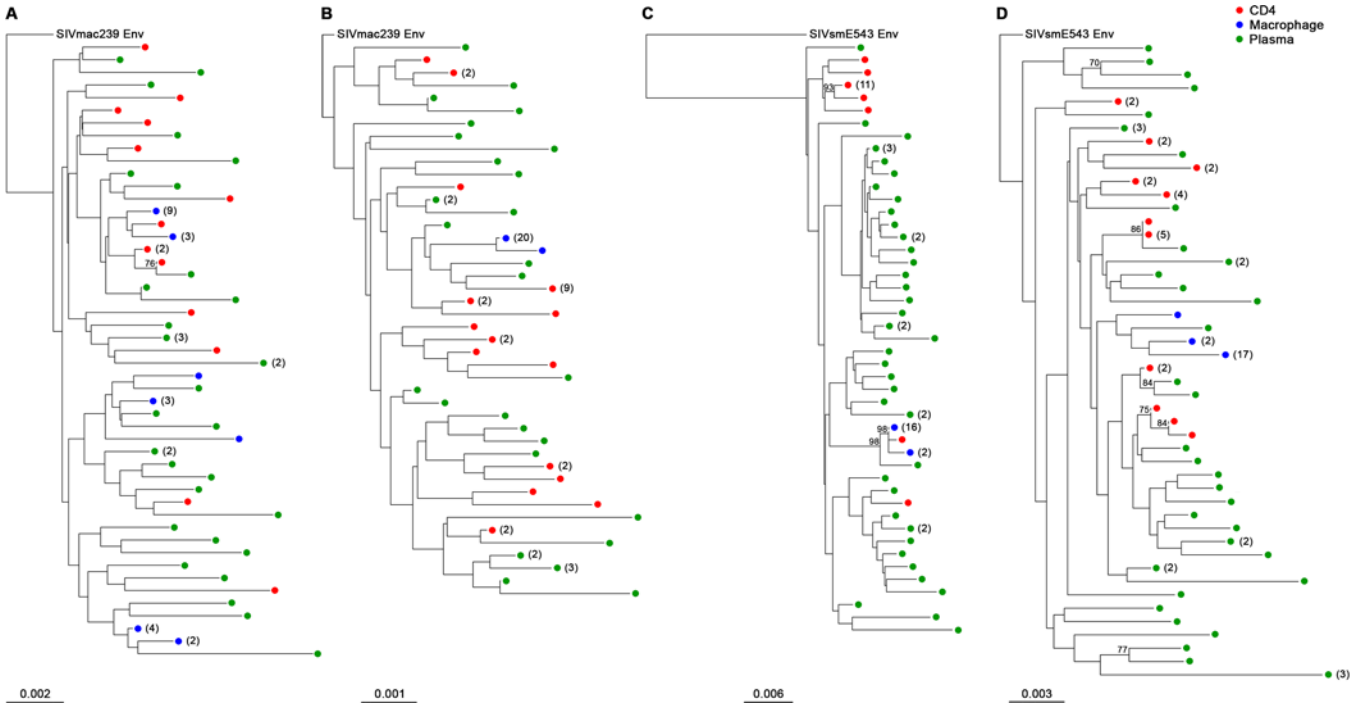

Figure 2. Phylogenetic distribution of *Env* sequences from co-culture and contemporaneous plasma. Viral RNA from cell culture media and necropsy plasma was isolated and sequenced for the variable regions 1–4 (V1–V4) of *Env*. Phylogenies constructed using the neighbor-joining method and Kimura 2-parameter model illustrate the genetic distribution of viruses from cocultures and plasma for each animal: (**A**) PT99P052, (**B**) RhDB92, (**C**) Rh848, and (**D**) Rh591. Identical sequences are grouped with the number of sequences indicated in parentheses. Sequence source is indicated by color: macrophage coculture (blue), $CD4^+$ T cell coculture (red), and contemporaneous plasma (green). Branch length is indicated per animal. Root SIV *Env* sequences were obtained from the NCBI Nucleotide database.

When comparing translated *Env* sequences from Rh591, differences between macrophage and $CD4^+$ T cell–associated sequences occurred primarily in V1/V2 and V4 (Figure 3). In a small set of sequences, mutations occurred in or around CD4 binding domain residues. These mutations were generally synonymous, mostly occurred in plasma *Env* sequences, and were not unique to macrophage coculture–derived sequences. Two plasma sequences and a $CD4^+$ T cell–associated *Env* sequence had a nonsilent mutation in a CD4 binding domain region that encoded aspartic acid instead of glutamic acid at residue 469 (DIDW not EIDW). Taken together, the macrophage-associated *Env* sequences did not have unique amino acid residues compared with plasma-associated or $CD4^+$ T cell–associated sequences, including mutations at potential N-linked glycosylation sites (no pattern for addition or loss of predicted glycosylation sites) (Figure 3). Thus, there was no indication that macrophage-associated sequences had modified CD4 binding domain regions compared with $CD4^+$ T cell–associated sequences or plasma *Env* sequences.

Viral DNA and rearranged TCR-γδ DNA in lymphoid myeloid cells from ARV-treated animals. After determining that lymphoid myeloid cells containing viral DNA can also contain replication-competent virus in ARV-naive animals, we next examined lymphoid tissue–resident myeloid cells from ARV-treated animals to investigate the potential role of myeloid cells in the latent viral reservoir. As previously described, we sorted memory $CD4^+$ T cells and myeloid cells from the spleen of Asian macaques who were infected with SIVmac239 and treated with ARV for at least 5 months (Table 1). When analyzed for viral DNA and rearranged TCR-γδ DNA levels by quantitative PCR (qPCR), 7 of the 17 ARV-treated animals had viral DNA^+ splenic myeloid cells (41%) (Figure 4A). While the frequency of animals with viral DNA^+ lymphoid myeloid cells is comparable to previously reported data for ARV-naive animals, there were some differences in the ARV-treated cohort compared with untreated animals. In ARV-treated animals, the levels of rearranged TCR-γδ DNA and SIV *Gag* DNA in myeloid cells were significantly decreased compared with untreated animals (SIV *Gag* $P = 0.017$, TCR-γδ $P < 0.0001$, Figure 4A).

As with the ARV-naive cohort, we next examined myeloid cells from the 7 ARV-treated animals with viral DNA^+ splenic myeloid cells for replication-competent virus via coculture with CEMx174

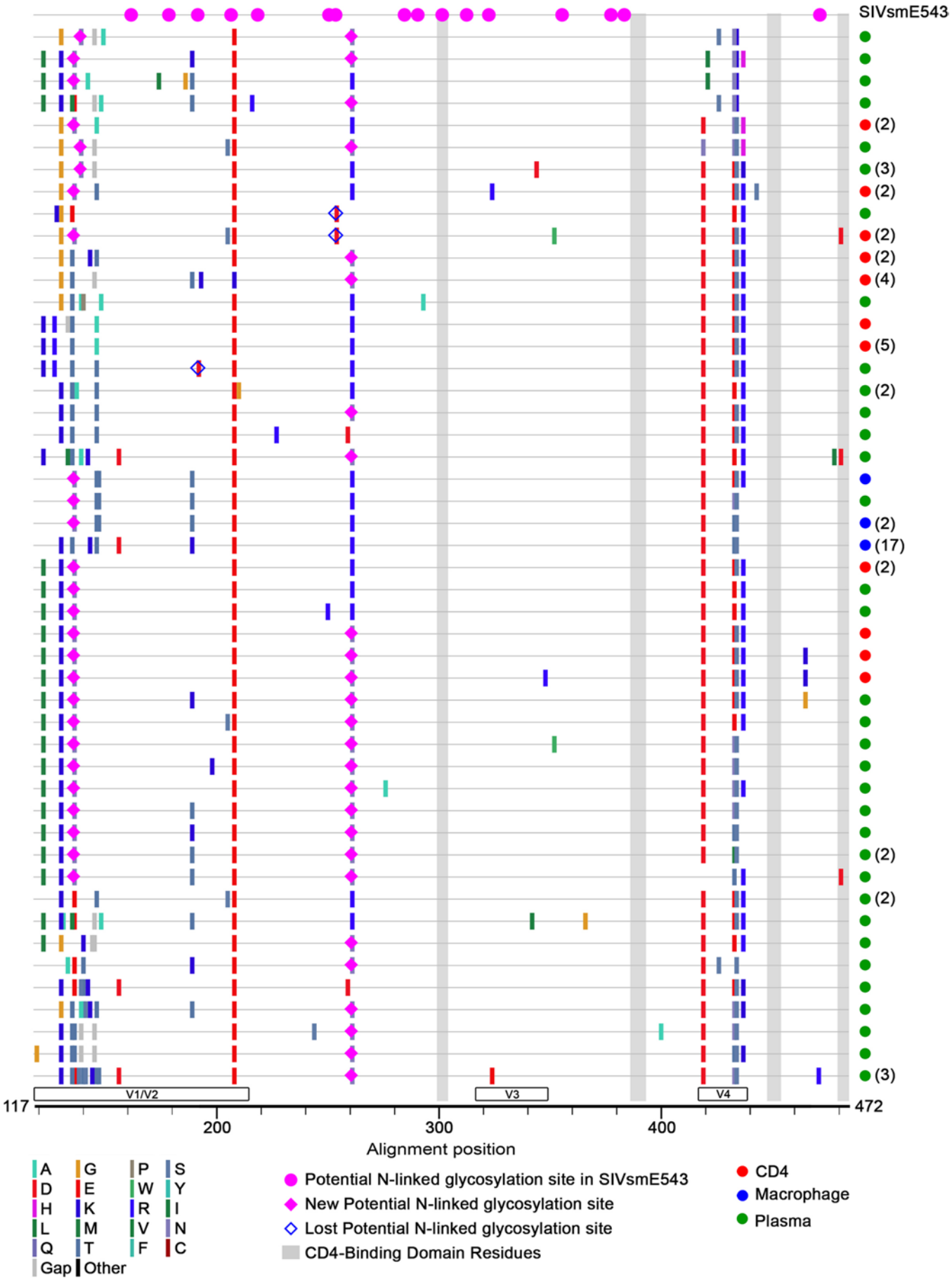
SIVsmE543
(2)
(3)
(2)
(2)
(2)
(4)
(5)
(2)
(2)
(17)
(2)
(2)
(2)
(3)
V1/V2
V3
V4
117
472
200
300
400
Alignment position
A
D
H
L
Q
Gap
G
E
K
M
T
Other
P
W
R
V
F
S
Y
I
N
C
Potential N-linked glycosylation site in SIVsmE543
New Potential N-linked glycosylation site
Lost Potential N-linked glycosylation site
CD4-Binding Domain Residues
CD4
Macrophage
Plasma

Figure 3. Alignment of translated *Env* sequences from Rh591. Potential N-linked glycosylation sites and variation in amino acid residues were identified by Highlighter analysis. CD4 binding domain residues are indicated with shaded boxes. Identical sequences were grouped with the number of sequences given in parentheses. Amino acid changes and potential glycosylation sites depicted as indicated in the legend. Sequence source is indicated by color: macrophage (blue), CD4+ T cell (red), and plasma (green). The SIVsmE543 master sequence was obtained from the NCBI Nucleotide database.

cells. In repeated trials with the same culture conditions used for cells sorted from ARV-naive animals, we were unable to detect replication-competent virus by ELISA for SIV p27 in the cell culture supernatant. Although activation of cells via xenographic interactions with CEMx174 cells in coculture was sufficient to stimulate viral replication in trials with ARV-naive animals, another group utilized TNF-α stimulation of macrophages in coculture with CEMx174 cells to promote viral replication (46). To determine whether additional stimulation was required to amplify replication-competent virus from myeloid cells of ARV-treated animals, we next cultured sorted splenic memory CD4+ T cells or myeloid cells with CEMx174 cells in the presence of staphylococcal enterotoxin B (SEB) or TNF-α, respectively. To reduce the likelihood that the lack of viral replication was a result of small sample bias, we also increased the scale of each coculture to 7.5×10^5 primary cells in each coculture well. For all 3 animals, coculture of memory CD4+ T cells with CEMx174 with SEB stimulation resulted in detectable SIV p27 Gag in cell culture media after 3 weeks (Figure 4B). In one animal, we also detected viral replication from unstimulated memory CD4+ T cell coculture after 3 weeks. However, none of the animals had detectable SIV p27 in cell culture media from myeloid cell cocultures with or without TNF-α stimulation after 3 weeks. Importantly, in total we cocultured 6 million splenic myeloid cells from 9 ARV-treated Asian macaques and were unable to rescue replication-competent virus, irrespective of stimulation method. From our previous experience in growing replication-competent virus from myeloid cells of ARV-naive animals, the levels of viral DNA in myeloid cells of ARV-treated animals should have been sufficient for us to detect replication-competent virus. Moreover, in determining which animals to analyze with the addition of TNF-α stimulation in macrophage cocultures, we selected the 3 ARV-treated animals with the highest levels of viral DNA in myeloid cells (0.2, 0.06, and 0.0005 copies of viral DNA/100 sorted macrophages). Given the lower myeloid cell viral DNA levels in the remaining ARV-treated animals and the absence of detectable replication-competent virus in macrophages from the 3 TNF-α–stimulated experiments, we concluded that using TNF-α stimulation for animals with significantly lower viral DNA levels would not yield productive results, as any replication-competent virus present would be at an exceedingly low frequency.

Viral DNA levels in lung CD4+ T cells and alveolar macrophages from ARV-treated HIV+ individuals. While the SIV/rhesus macaque system is an effective model for HIV, SIV and HIV have several inherent differences, and results observed in macaques do not always translate directly to humans. Therefore, to determine if phagocytosis of infected CD4+ T cells might also occur in HIV-infected individuals, we sorted memory CD4+ T cells and alveolar macrophages from the BAL of 9 HIV-infected individuals treated with ARVs for 3 years (Table 2). Importantly, BAL is a fairly routine procedure in humans where isolation of high numbers (millions) of tissues macrophages is possible. We have had previous success in performing experiments with alveolar macrophages and BAL-resident T cells (33, 47). Plasma viremia was undetectable in 6 of these individuals and 1 patient maintained significant levels of plasma viremia. Upon flow cytometric analysis, HIV *Gag* DNA was detected in memory CD4+ T cells from 4 individuals (44%) and in alveolar macrophages from only 1 individual (11%) (Figure 5). Given that this qPCR assay is sensitive to 1 copy of viral DNA per reaction (48) and that we were able to sort approximately 1 million alveolar macrophages from each BAL sample, the low frequency of viral DNA+ alveolar macrophages is unlikely to be due to insufficient sensitivity. Although we were able to sort

Table 2. Study patient characteristics

Patient ID	CD4+ T Cells[A]	Viral Load[B]	ARV Duration[C]
3003	140	49,100	1,000
3008	529	308	1,000
3014	421	Undetected	1,000
3015	826	Undetected	1,000
3016	299	407	1,000
3018	670	Undetected	1,000
3020	393	Undetected	1,000
3025	374	Undetected	1,000
3028	370	Undetected	1,000

[A]Number of CD4+ T cells/μl blood. [B]Copies viral RNA/ml of plasma. [C]Antiretroviral (ARV) duration in days.

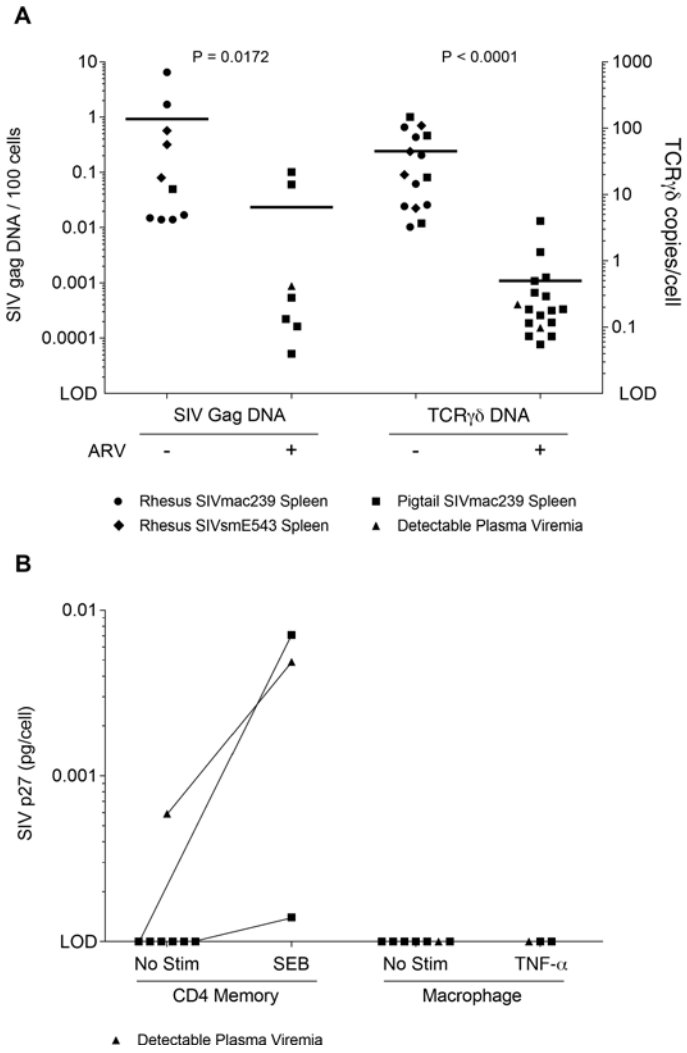

Figure 4. Viral DNA, rearranged TCR DNA, and replication-competent SIV in ARV-treated macaques. (**A**) Viral DNA (left) and rearranged TCR-γδ DNA (right) levels in splenic myeloid cells of antiretroviral-treated (ARV-treated) animals and ARV-naive animals via Mann-Whitney tests (ARV-treated $n = 17$, ARV-naive $n = 28$, qPCR in duplicate). (**B**) Memory CD4$^+$ T cells (left) or myeloid cells (right) from ARV-treated animals were cocultured with CEMx174 cells and analyzed for SIV p27 with ELISA after 3 weeks. Reported values are pg SIV p27 per primary cell in coculture (7.5×10^5 sorted cells per well).

millions of alveolar macrophages (8×10^5 to 1.3×10^6 cells per person), CD4$^+$ T cell counts in BAL were significantly lower and may account for the lower frequency of individuals with viral DNA$^+$ CD4$^+$ T cells from BAL. Indeed, some individuals with very low numbers of sorted CD4$^+$ T cells (i.e., 1,000 cells) had undetectable viral DNA. Rearranged TCR-γδ DNA was detectable at low levels in alveolar macrophages from all but 1 individual. Importantly, the only individual with detectable viral DNA within alveolar macrophages (patient 3016) had ongoing viral replication and evidence of T cell phagocytosis with 0.3 copies of TCR DNA per myeloid cell. Thus, we did not find evidence that alveolar macrophages could represent a viable viral reservoir.

Discussion

We previously showed that lymphoid tissue–resident myeloid cells can contain SIV DNA and that these cells may acquire viral DNA via phagocytosis of infected CD4$^+$ T cells (43). Here, we have isolated lymphoid tissue–resident myeloid cells and memory CD4$^+$ T cells from the same tissue of SIV-infected Asian macaques to examine whether myeloid cells contain replication-competent virus in ARV-naive and ARV-treated animals and, consequently, whether these cells are a potential reservoir of latent virus. We found that (a) in untreated animals, lymphoid tissue–resident macrophages with detectable SIV DNA can also contain replication-competent virus; (b) the replication-competent virus isolated from myeloid cell cocultures is genetically similar to virus isolated from cocultures of memory CD4$^+$ T cells from the same tissue; (c) myeloid cells isolated from the spleen of SIV-infected animals on ARVs for at least 5 months had viral DNA in 40% of animals; (d) levels of viral DNA and rearranged TCR DNA were decreased in ARV-treated animals compared with untreated animals; (e) we were unable to rescue replication-competent virus from splenic myeloid cells of ARV-treated animals; and (f) we did not observe viral DNA in alveolar macrophages taken from BAL of HIV-infected individuals on ARVs with undetectable plasma viremia.

Several SIV models have been used to examine infection of myeloid cells in vivo. However, the models wherein macrophages are routinely infected in vivo are generally characterized by massive CD4$^+$ T cell depletion and highly accelerated disease progression (reviewed in detail in ref. 40). For example, Avalos et al. used a dual-infection model with a highly CD4-tropic virus (SIV/17E-Fr) and a neurotropic SIV swarm (SIV/DeltaB760) where CD4$^+$ T cells are dramatically depleted early in infection. In this model, the authors demonstrated that splenic macrophages contain replication-competent virus ex vivo when stimulated in coculture (46). While these results show that splenic macrophages can support viral replication, applying these findings to HIV disease progression is unclear given the accelerated disease progression and rapid CD4$^+$ T cell loss, both of which are only rarely observed in HIV infection. Others have demonstrated macrophage infection in animals with very low CD4$^+$ T cell counts by depleting CD4$^+$ T cells with an anti-CD4 antibody and examining tissue macrophages for viral RNA by in situ hybridization and immunohistochemistry (39, 49). While these studies showed the potential for viral replication in myeloid cells, the infected myeloid cells had a short half-life in vivo and, again, the animals exhibited accelerated disease progression.

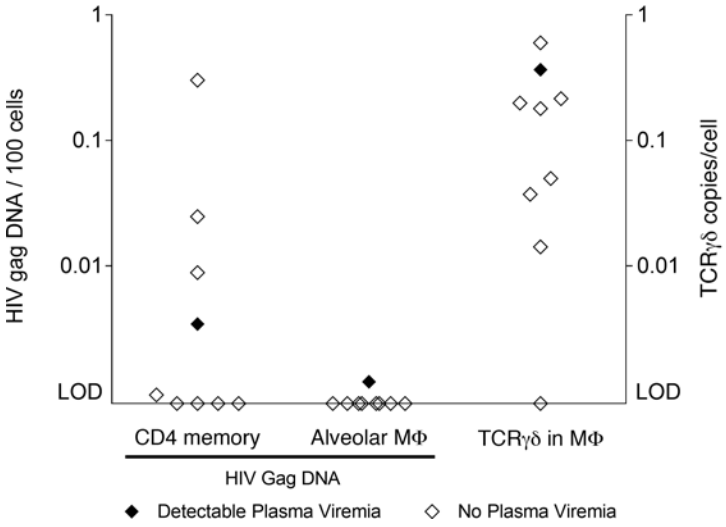

Figure 5. Viral DNA and TCR DNA in BAL of HIV⁺ individuals on ARVs. HIV *Gag* DNA levels in memory CD4⁺ T cells (left) and alveolar macrophages (MΦ, middle) sorted from bronchoalveolar lavage (BAL) of HIV⁺ individuals on antiretrovirals (ARVs) for 3 years. Alveolar macrophages were also analyzed for rearranged TCR DNA content via qPCR (right).

Here, we have examined myeloid cells from animals that were infected with 1 of the 2 most conventional SIV strains that more closely follow patterns of HIV infection. Our animals had a range of viral loads and CD4⁺ T cell counts, and were sacrificed at varying stages of disease progression. We found that lymphoid tissue–resident myeloid cells can contain replication-competent virus in ARV-naive animals when the myeloid cells contain viral DNA. Given that the levels of SIV detected in cell culture media were lower in myeloid cell cocultures than memory CD4⁺ T cell cocultures of cells isolated from the same tissue, the frequency of myeloid cells containing replication-competent virus was significantly lower than that of memory CD4⁺ T cells in the same tissue and consequently limited our ability to sequence high numbers of viral clones within myeloid cells.

Our phylogenetic analysis indicates that the viruses isolated from CD4⁺ T cell coculture, macrophage coculture, and contemporaneous plasma are genetically similar within each animal. Although posterior probability analysis indicated that sequences from memory CD4⁺ T cells and macrophages were statistically different in 1 animal (Rh591), several factors limit a conclusion that replication-competent viruses in macrophages differ from viruses from CD4⁺ T cells in the same tissue. First, bootstrap analysis of each tree indicates limited significance of branching at most nodes in each tree, suggesting that genetic differences between sequences were minor and insufficient for strong phylogenetic distinction. Second, the nonsynonymous mutations observed were not unique to macrophage-associated *Env* sequences and do not correspond to commonly referenced macrophage-tropic modifications. For example, the translated macrophage-associated Env sequences from Rh591 do not contain amino acid changes homologous to E153G and D167N, D178G, N197D, V200T, N283, or N386D in HIV (50–54). Conversely, all of the Env sequences from Rh591 contain an asparagine residue homologous to N173, which is associated with reduced macrophage infectivity in SIVmac251 and SIVmac239 (55, 56). Although HIV and SIV have varying distributions of potential N-linked glycosylation sites and other structural differences, the absence of major macrophage-tropic residues in sequences from Rh591 suggest that any statistical differentiation between macrophage and memory CD4⁺ T cell–associated *Env* sequences is not indicative of a developing macrophage tropism.

Although memory CD4⁺ T cells have been identified as the predominant reservoir of latent viral infection (1), investigating the potential role for tissue-resident macrophages in the latent viral reservoir is crucial for understanding latent viral infection persistence in ARV-treated individuals. Here, we examined splenic tissue from 17 ARV-treated pigtail macaques infected with SIVmac239 for viral DNA content and evidence of T cell phagocytosis. The frequency of animals with viral DNA⁺ myeloid cells was similar in the ARV-treated cohort (7 of 17, 41%) compared with previously reported data from ARV-naive animals (10 of 25, 40%) (43). Although the number of animals with viral DNA⁺ splenic myeloid cells was comparable in ARV-naive and -treated animals, levels of detected viral DNA and rearranged TCR-γδ DNA were significantly reduced in the ARV-treated animals and we could not rescue replication-competent virus in splenic myeloid cells from ARV-treated animals. While we cannot conclude that myeloid cells contain absolutely no replication-competent virus in ARV-treated animals, these results indicate that splenic myeloid cells are not a significant source of latent virus. Moreover, undetectable levels of replication-competent virus in ARV-treated animals may be explained in part by turnover of SIV⁺ myeloid cells during ARV therapy (49).

Overall, our results are consistent with macrophage phagocytosis of infected CD4⁺ T cells being an important route for myeloid cell acquisition of virus in lymphoid tissues. The genetic similarity between macrophage-associated and CD4⁺ T cell–associated sequences suggests that lymphoid tissue–resident macrophages are not preferentially infected with macrophage-tropic viruses and that macrophages may acquire

HIV/SIV directly from $CD4^+$ T cells in the surrounding tissue. In addition, the lower levels of viral DNA and TCR-γδ DNA in splenic macrophages from ARV-treated animals may reflect an overall reduction in $CD4^+$ T cell death from viral replication and, consequently, less frequent phagocytosis of dead or dying infected $CD4^+$ T cells. Assessing mechanisms for HIV/SIV infection via phagocytosis requires further investigation, as HIV/SIV may infect macrophages in lymphoid tissues via other interactions with $CD4^+$ T cells such as cell-to-cell transmission or infection from virus replicating in $CD4^+$ T cells (40, 57).

While several SIV models have been used to study infection of tissue-resident macrophages, analysis of HIV infection of macrophages (in vivo or ex vivo) is more limited largely due to challenges in sample collection from HIV-infected individuals. Many years ago, one group obtained spleen samples from HIV-infected patients (removed for other medical reasons) and found 20- to 100-fold lower levels of viral DNA in macrophages compared with $CD4^+$ T cells (58). A more commonly sampled site for HIV-infected individuals is BAL. Two studies found that 70% of HIV-infected individuals had low levels of viral DNA in alveolar macrophages (32, 33). Citing the low levels of viral DNA detected in alveolar macrophages in these studies, the authors noted the possibility of contaminating HIV^+ $CD4^+$ T cells in the alveolar macrophage population and the difficulties in purely isolating alveolar macrophages due to autofluorescence and/or nonspecific antibody binding. Moreover, alveolar macrophages may phagocytose HIV/SIV–infected $CD4^+$ T cells in the lungs. Indeed, that we found evidence for $CD4^+$ T cell phagocytosis by alveolar macrophages and only found viral DNA in alveolar macrophages of one individual who had ongoing viral replication suggest that if these cells harbor latent virus, it is at very low levels considering that we flow cytometrically sorted more than 3 million alveolar macrophages cumulatively from these subjects.

Investigation of HIV/SIV infection of tissue-resident macrophages was limited to the spleen, mesenteric lymph nodes, and BAL in this study. However, further examination of brain microglial cells and perivascular macrophages in HIV/SIV infection is also necessary to characterize the latent viral reservoir. This includes determining whether brain-resident macrophages harbor replication-competent virus in vivo and investigating how they acquire HIV/SIV — in particular understanding the contributions of direct infection, clearance of viral immune complexes, and potential phagocytosis of infiltrating infected $CD4^+$ T cells. One potential mechanism for acquisition of viral DNA and antigen in the brain, where $CD4^+$ T cells are scarce, may be phagocytosis of antibody/complement–opsonized virions in a manner similar to follicular dendritic cell phagocytosis of viral immune complexes in lymph node B cell follicles (or tethering of opsonized virions extracellularly) (59–61). Recent identification of meningeal lymphatic vessels in the brain has further complicated questions about viral entry into the brain (19, 62). For example, a recent study detected HIV p24 in macrophages lining meningeal lymphatic vessels but also observed that the detected viral sequence was not compartmentalized and originated from the patient's lymph node (19). New models, including a novel SHIV that induces encephalitis and brain macrophage infection (63), could help address these questions, although studies using canonical SIV may offer more representative disease pathogenesis. Indeed, significant advances in developing a conventionally progressing neuroAIDS model of SIVsmE543 have been made (20–22). Ongoing work characterizing SIV in brain-resident macrophages using a conventionally progressive neuroAIDS animal model may help address some of these outstanding questions, including whether brain macrophages harbor replication-competent virus in ARV-naive and ARV-treated animals.

In conclusion, we have found that (a) in untreated animals, lymphoid tissue–resident macrophages with detectable SIV *Gag* DNA can also contain replication-competent virus; (b) the replication-competent virus isolated from myeloid cell cocultures is genetically similar to virus isolated from cocultures of memory $CD4^+$ T cells from the same tissue; (c) myeloid cells isolated from the spleen of SIV-infected animals on ARVs for at least 5 months had viral DNA in 40% of animals; (d) levels of viral DNA and rearranged TCR DNA were decreased in ARV-treated animals compared with untreated animals; (e) we were able to detect replication-competent virus in memory $CD4^+$ T cell cocultures of cells from ARV-treated animals but were unable to rescue replication-competent virus from splenic myeloid cells of ARV-treated animals; and (f) in BAL from HIV-infected individuals treated with ARVs for 3 years, 44% of individuals had viral DNA in memory $CD4^+$ T cells and 11% had viral DNA in alveolar macrophages. Taken together, these results suggest that viral DNA^+ lymphoid myeloid cells can contain replication-competent virus in the absence of ARV treatment, that this acquisition of virus can involve phagocytosis of infected $CD4^+$ T cells, and that ARV treatment reduces the pool of replication-competent virus in both memory $CD4^+$ T cells and myeloid cells. Therefore, macrophages in lymphoid tissue and BAL are likely not a significant source of latent virus in vivo.

Methods

Animals. To characterize and determine the cellular targets for SIV in vivo, we studied tissues from a diverse cohort of SIV-infected rhesus macaques (RMs) and pigtailed macaques (PTMs). Tissues were obtained at necropsy from 26 RMs (*Macaca mulatta*) and 19 PTMs (*Macaca nemestrina*) at a variety of times after infection with SIVmac239 or SIVsmE543 (Table 1). Animals with simian AIDS were diagnosed by opportunistic infections, lymphomas, or greater than 15% body weight loss.

Human subjects. The pulmonary immune reconstitution inflammatory syndrome (IRIS) study is an ongoing, prospective observational study designed to assess protective and pathological immune responses in the lung after HAART initiation. HIV-infected subjects who planned to initiate HAART based on clinical criteria were asked to undergo bronchoscopy before initiating treatment, 1 month, and 1 year after treatment initiation. Nine HIV-infected subjects who were more than 18 years of age and free of acute respiratory tract symptoms were recruited for this study. Subjects had received combination antiretroviral therapy for 36 months. Clinical details are shown in Table 2. HAART regimens were not dictated by protocol, but no patient received a CCR5 antagonist. Viral load was determined using either the Roche Amplicor Monitor assay or the Roche Ultradirect assay.

Cell isolation/sorting. Splenic and mesenteric lymph node macrophages and lymphocytes were isolated after tissue digestion. Splenic cell suspensions were treated with ACK lysis buffer (Lonza) after digestion. In some cases single-cell suspensions were cryopreserved.

Flow cytometry. The SIV infection frequency of memory $CD4^+$ T cells and myeloid cells was determined by flow cytometrically sorting each subset followed by qPCR for viral DNA. Memory $CD4^+$ T cells were defined as live, $CD45^+CD3^+CD4^+CD95^+$ lymphocytes; myeloid cells were defined as live, $CD45^+CD3^-CD20^-NKG2A^-CD11b^+$ and or $CD14^+$ (Supplemental Figure 1). Cells were stained with the live/dead exclusion dye Aqua blue (Invitrogen) and then with antibodies against CD3 (clone SP34-2), CD4 (clone L200), CD95 (clone DX2), CD8 (clone SK8), CD20 (clone L27), HLADR (clone L243), CD14 (clone M5E2), CD45 (clone D058-1283) (all BD Pharmingen); CD28 (clone CD28.2, Beckman Coulter), NKG2A (clone Z199, Beckman Coulter); and CD11b (clone ICRF44, BioLegend). Memory $CD4^+$ T cells and alveolar macrophages from BAL from humans were flow cytometrically sorted. Memory $CD4^+$ T cells were defined as above and alveolar macrophages were sorted based upon characteristic forward-scatter and side-scatter properties as previously described (33). In our experience, alveolar macrophages cannot be reliably phenotyped using flow cytometry because of their extremely high autofluorescence.

Cell coculture for detection of replication-competent virus. Viably sorted cells were cultured with CEMx174 cells (NIH AIDS Reagent Program, lot 130358) in complete RPMI — RPMI-1640 (HyClone) supplemented with 10% heat-inactivated fetal bovine serum (Hyclone), 2 mM L-glutamine (Gibco), and penicillin/streptomycin (Gibco). Five-fold dilutions of sorted cells (from 4×10^4 to 320 cells) were cultured in triplicate with 5×10^4 CEMx174 cells in 96-well round-bottom plates (Corning). Cell cultures were split 1:4 on days 3, 7, 10, 14, 17, and 21. Cell culture media samples were collected on days 7, 14, and 21. Cell culture media were analyzed for virus content via a commercially available ELISA for SIV p27 Gag (Advanced Bioscience Laboratories) according to the manufacturer's instructions. Results were reported as pg SIV p27 per cell, where cell number is the number of primary cells in the tested coculture well.

Coculture of stimulated cells from ARV-treated animals. Memory $CD4^+$ T cells and myeloid cells were sorted from the spleens of ARV-treated animals as described above. Sorted cells (7.5×10^5) were cultured with 1×10^6 CEMx174 cells in 6-well plates with complete RPMI. Cocultures with memory $CD4^+$ T cells were stimulated with 1 μg/ml *Staphylococcus aureus* enterotoxin B (SEB) (Sigma-Aldrich) or were cultured without stimulation. Cocultures with macrophages were stimulated with 10 ng/ml recombinant human TNF-α (R&D Systems). After 4 days in culture, well volume was brought to the original culture volume by adding complete RPMI containing the corresponding stimulant. Cell culture media samples were collected on days 7, 14, and 28. After day 4, well volume was maintained with complete RPMI without additional stimulant added. Cell culture media were analyzed for virus content via the SIV p27 Gag ELISA according to the manufacturer's instructions. Results were reported as pg SIV p27 per cell, where cell number is the number of primary cells in the tested coculture well.

Sequencing of viral RNA in plasma and cell culture media. Viral RNA was extracted from cell culture media or necropsy plasma using the QIAamp Viral RNA Mini Kit (QIAGEN). cDNA from cell culture media was synthesized using random hexamers and the SuperScript III First-Strand Synthesis Kit (Invitrogen). Reverse transcription of plasma viral RNA was performed using the Thermoscript RT-PCR System (Invitrogen)

and gene-specific primers for either SIVsmE543 or SIVmac239 as previously described (64, 65). The V1–V4 region of the viral *Env* gene was amplified by PCR using Platinum Taq High Fidelity DNA polymerase (Invitrogen). SIVmac239 *Env* sequences were amplified using the primer pair Env239F (5′-GCCTTGTGTA-AAATTATCCCCA-3′) and Env239R (5′-CTTGAGGTGCCACCAGTAGT-3′). SIVsmE543 *Env* sequences were amplified using the primer pair Env543F (5′-GCCCTGTGTAAAACTTACCCCA-3′) and Env543R (5′-CTTGAGGCACCAGTTGTGGT-3′). Amplicons were ligated into the pGEM-T Easy Vector (Promega) and transformed into DH5α *E. coli* competent cells. Selected colonies were amplified using Platinum Taq High Fidelity DNA polymerase with M13 universal primers (66). Sanger sequencing analysis was performed by Beckman Coulter Genomics or Genewiz. Consensus sequences were aligned using Sequencher 5.4 (Gene Codes Corporation).

Sequence analysis and phylogenetic tree construction. Multiple sequence alignments of the *Env* consensus sequences were constructed using the ClustalW method and MacVector 14.5.3. Sequences with missense mutations or large deletions/insertions were omitted. Sequences with 1 to 2 base pair differences were considered identical clones and combined for phylogenetic tree construction, with the number of sequences per clone indicated in parentheses. Phylogenetic trees were constructed using the Kimura 2-parameter model and neighbor-joining method. Bootstrap analysis was performed with 1,000 replications. Aligned *Env* sequences for Rh591 were translated using the Codon Alignment v2.1.0 tool and analyzed for amino acid mismatches and potential N-linked glycosylation sites using Highlighter (Los Alamos National Labs HIV Database, http://www.hiv.lanl.gov/) (67). Root SIV *Env* sequences for SIVsmE543 and SIVmac239 were obtained from the NCBI nucleotide database (U72748.2 and AY588946.1, respectively).

Quantification of cell-associated viral DNA. Cell subsets were sorted using a FACSAria II with FACSDiva software (BD Pharmingen). Sorted cells were then lysed using 25 μl of a 1:100 dilution of proteinase K (Roche) in 10 mM Tris buffer. qPCR was performed using 5 μl of cell lysates per reaction. Reaction conditions were as follows: 95°C holding stage for 5 minutes, and 50 cycles of 95°C for 15 seconds followed by 60°C for 1 minute using the TaqMan Gene Expression Master Mix (Applied Biosystems). SIVmac239 *Gag* was amplified using the primer/probe set (forward primer 5′-GTCTGCGTCATYTGGTGCATTC-3′, reverse primer 5′-CACTAGYTGTCTCTGCACTATRTGTTTTG-3′ and probe 5′-CTTCRTCAGTYT-GTTTCACTTTCTCTTCTGCG-3′). SIVsmE543 *Gag* was amplified using the primer/probe set (forward primer 5′-GGCAGGAAAATCCCTAGCAG-3′, reverse primer 5′-GCCCTTACTGCCTTCACTCA-3′, and probe 5′-AGTCCCTGTTCRGGCGCCAA-3′). HIV *Gag* was amplified using the sequence probe set (forward primer 5′-GGTGCGAGAGCGTCAGTATTAAG-3′, reverse primer 5′-AGCTCCCTGCTT-GCCCATA-3′, and probe 5′-AAAATTCGGTTAAGGCCAGGGGGAAAGAA-3′). For cell number quantification, monkey or human albumin was measured as previously described (68). The instrument used for all real-time PCR was the StepOne Plus (Applied Biosystems) and the analysis was performed using StepOne software (Applied Biosystems).

Rearranged TCR DNA quantification. Cells were sorted and lysed as described above, and real-time TCR qPCR was performed. Reaction conditions were as follows: 95°C holding stage for 7 minutes, followed by 45 cycles at 95°C for 45 seconds, 60°C for 1 minute, and 72°C for 90 seconds. Rearranged TCRG DNA detection was accomplished using a proprietary mix of unlabeled TCRG primers (Invivoscribe), AmpliTaq Gold Polymerase (Applied Biosystems), and SYBR Green I dye (Invitrogen) (69).

Plasma viral loads. Plasma samples were analyzed for SIV RNA using a fluorescence resonance energy transfer probe–based real-time RT-PCR (Taqman) assay that provides a threshold sensitivity of 10 copy Eq/ml, as previously described (70). All PCR reactions were run on an ABI Prism 7700 Sequence Detection System and the fluorescent signal-based quantification of viral RNA copy numbers in test samples was determined by ABI Sequence Detection System software (Applied Biosystems).

Statistics. Statistical analysis was performed with GraphPad Prism Version 6 or 7 using the Mann-Whitney *t* test. Posterior probability to assess sequence differences was performed as previously described (71).

Study approval. Animals were housed and cared for in accordance with American Association for Accreditation of Laboratory Animal Care (AAALAC) standards in AAALAC-accredited facilities, and all animal procedures were performed according to protocols approved by the IACUC of the National Institute of Allergy and Infectious Diseases (NIAID) under animal study protocols LPD 26 and LMM6. The IRIS study was approved by the IRB at Indiana University under study number 0510-12 and all subjects provided written informed consent.

Author contributions

SD, JB, and VM designed the research study. AO, FW, and KM contributed to the animal studies and sample processing. SD and JB supervised the projects, conducted the experiments, analyzed the data, and wrote the manuscript. HT and KK provided human BAL samples.

Acknowledgments

We would like to acknowledge Heather Cronise, JoAnne Swerczek, Richard Herbert, and all the veterinary staff at the NIH animal center. We would like to thank CLIC/BBC for advice and helpful discussions. We would like to thank Brandon Keele and Bernard Lafont for assistance in analyzing SIV *Env* sequencing data. Funding for this study was provided in part by the Division of Intramural Research/NIAID/NIH. The content of this publication does not necessarily reflect the views or policies of the Department of Health and Human Services, nor does the mention of trade names, commercial products, or organizations imply endorsement by the U.S. Government.

Address correspondence to: Jason M. Brenchley, 4 Center Drive Room 201, 9000 Rockville Pike, Bethesda, Maryland 20892, USA. Phone: 301.496.1498; E-mail: jbrenchl@mail.nih.gov.

1. Murray AJ, Kwon KJ, Farber DL, Siliciano RF. The latent reservoir for HIV-1: how immunologic memory and clonal expansion contribute to HIV-1 persistence. *J Immunol*. 2016;197(2):407–417.
2. Davey RT, et al. HIV-1 and T cell dynamics after interruption of highly active antiretroviral therapy (HAART) in patients with a history of sustained viral suppression. *Proc Natl Acad Sci USA*. 1999;96(26):15109–15114.
3. Chun TW, et al. Rebound of plasma viremia following cessation of antiretroviral therapy despite profoundly low levels of HIV reservoir: implications for eradication. *AIDS*. 2010;24(18):2803–2808.
4. Rothenberger MK, et al. Large number of rebounding/founder HIV variants emerge from multifocal infection in lymphatic tissues after treatment interruption. *Proc Natl Acad Sci USA*. 2015;112(10):E1126–E1134.
5. Jenkins SJ, et al. Local macrophage proliferation, rather than recruitment from the blood, is a signature of TH2 inflammation. *Science*. 2011;332(6035):1284–1288.
6. Schulz C, et al. A lineage of myeloid cells independent of Myb and hematopoietic stem cells. *Science*. 2012;336(6077):86–90.
7. Saijo K, Glass CK. Microglial cell origin and phenotypes in health and disease. *Nat Rev Immunol*. 2011;11(11):775–787.
8. Filipowicz AR, et al. Proliferation of perivascular macrophages contributes to the development of encephalitic lesions in HIV-infected humans and in SIV-infected macaques. *Sci Rep*. 2016;6:32900.
9. Gartner S, Markovits P, Markovitz DM, Kaplan MH, Gallo RC, Popovic M. The role of mononuclear phagocytes in HTLV-III/LAV infection. *Science*. 1986;233(4760):215–219.
10. Koenig S, et al. Detection of AIDS virus in macrophages in brain tissue from AIDS patients with encephalopathy. *Science*. 1986;233(4768):1089–1093.
11. Wiley CA, Schrier RD, Nelson JA, Lampert PW, Oldstone MB. Cellular localization of human immunodeficiency virus infection within the brains of acquired immune deficiency syndrome patients. *Proc Natl Acad Sci USA*. 1986;83(18):7089–7093.
12. Ranki A, et al. Abundant expression of HIV Nef and Rev proteins in brain astrocytes in vivo is associated with dementia. *AIDS*. 1995;9(9):1001–1008.
13. Mack KD, et al. HIV insertions within and proximal to host cell genes are a common finding in tissues containing high levels of HIV DNA and macrophage-associated p24 antigen expression. *J Acquir Immune Defic Syndr*. 2003;33(3):308–320.
14. Salemi M, Lamers SL, Yu S, de Oliveira T, Fitch WM, McGrath MS. Phylodynamic analysis of human immunodeficiency virus type 1 in distinct brain compartments provides a model for the neuropathogenesis of AIDS. *J Virol*. 2005;79(17):11343–11352.
15. Kaul M, Garden GA, Lipton SA. Pathways to neuronal injury and apoptosis in HIV-associated dementia. *Nature*. 2001;410(6831):988–994.
16. Tornatore C, Chandra R, Berger JR, Major EO. HIV-1 infection of subcortical astrocytes in the pediatric central nervous system. *Neurology*. 1994;44(3 Pt 1):481–487.
17. Fischer-Smith T, Bell C, Croul S, Lewis M, Rappaport J. Monocyte/macrophage trafficking in acquired immunodeficiency syndrome encephalitis: lessons from human and nonhuman primate studies. *J Neurovirol*. 2008;14(4):318–326.
18. Thompson KA, Cherry CL, Bell JE, McLean CA. Brain cell reservoirs of latent virus in presymptomatic HIV-infected individuals. *Am J Pathol*. 2011;179(4):1623–1629.
19. Lamers SL, et al. The meningeal lymphatic system: a route for HIV brain migration? *J Neurovirol*. 2016;22(3):275–281.
20. Matsuda K, et al. Enhanced antagonism of BST-2 by a neurovirulent SIV envelope. *J Clin Invest*. 2016;126(6):2295–2307.
21. Matsuda K, et al. Characterization of simian immunodeficiency virus (SIV) that induces SIV encephalitis in rhesus macaques with high frequency: role of TRIM5 and major histocompatibility complex genotypes and early entry to the brain. *J Virol*. 2014;88(22):13201–13211.
22. Matsuda K, et al. Laser capture microdissection assessment of virus compartmentalization in the central nervous systems of macaques infected with neurovirulent simian immunodeficiency virus. *J Virol*. 2013;87(16):8896–8908.
23. Schnell G, Joseph S, Spudich S, Price RW, Swanstrom R. HIV-1 replication in the central nervous system occurs in two distinct cell types. *PLoS Pathog*. 2011;7(10):e1002286.
24. Sturdevant CB, et al. Central nervous system compartmentalization of HIV-1 subtype C variants early and late in infection in

young children. *PLoS Pathog*. 2012;8(12):e1003094.
25. Joseph SB, et al. Quantification of entry phenotypes of macrophage-tropic HIV-1 across a wide range of CD4 densities. *J Virol*. 2014;88(4):1858–1869.
26. Sturdevant CB, Joseph SB, Schnell G, Price RW, Swanstrom R, Spudich S. Compartmentalized replication of R5 T cell-tropic HIV-1 in the central nervous system early in the course of infection. *PLoS Pathog*. 2015;11(3):e1004720.
27. Tyor W, Fritz-French C, Nath A. Effect of HIV clade differences on the onset and severity of HIV-associated neurocognitive disorders. *J Neurovirol*. 2013;19(6):515–522.
28. McArthur JC, Steiner J, Sacktor N, Nath A. Human immunodeficiency virus-associated neurocognitive disorders: Mind the gap. *Ann Neurol*. 2010;67(6):699–714.
29. Sacktor N, Robertson K. Evolving clinical phenotypes in HIV-associated neurocognitive disorders. *Curr Opin HIV AIDS*. 2014;9(6):517–520.
30. Nau R, Sörgel F, Eiffert H. Penetration of drugs through the blood-cerebrospinal fluid/blood-brain barrier for treatment of central nervous system infections. *Clin Microbiol Rev*. 2010;23(4):858–883.
31. Cribbs SK, Lennox J, Caliendo AM, Brown LA, Guidot DM. Healthy HIV-1-infected individuals on highly active antiretroviral therapy harbor HIV-1 in their alveolar macrophages. *AIDS Res Hum Retroviruses*. 2015;31(1):64–70.
32. Lewin SR, Kirihara J, Sonza S, Irving L, Mills J, Crowe SM. HIV-1 DNA and mRNA concentrations are similar in peripheral blood monocytes and alveolar macrophages in HIV-1-infected individuals. *AIDS*. 1998;12(7):719–727.
33. Brenchley JM, et al. High frequencies of polyfunctional HIV-specific T cells are associated with preservation of mucosal CD4 T cells in bronchoalveolar lavage. *Mucosal Immunol*. 2008;1(1):49–58.
34. Yukl SA, et al. The distribution of HIV DNA and RNA in cell subsets differs in gut and blood of HIV-positive patients on ART: implications for viral persistence. *J Infect Dis*. 2013;208(8):1212–1220.
35. Fultz PN, McClure HM, Anderson DC, Switzer WM. Identification and biologic characterization of an acutely lethal variant of simian immunodeficiency virus from sooty mangabeys (SIV/SMM). *AIDS Res Hum Retroviruses*. 1989;5(4):397–409.
36. Zink MC, et al. High viral load in the cerebrospinal fluid and brain correlates with severity of simian immunodeficiency virus encephalitis. *J Virol*. 1999;73(12):10480–10488.
37. Igarashi T, et al. Rapid and irreversible $CD4^+$ T-cell depletion induced by the highly pathogenic simian/human immunodeficiency virus SHIV(DH12R) is systemic and synchronous. *J Virol*. 2002;76(1):379–391.
38. Shibata R, et al. Isolation and characterization of a syncytium-inducing, macrophage/T-cell line-tropic human immunodeficiency virus type 1 isolate that readily infects chimpanzee cells in vitro and in vivo. *J Virol*. 1995;69(7):4453–4462.
39. Ortiz AM, et al. Depletion of $CD4^+$ T cells abrogates post-peak decline of viremia in SIV-infected rhesus macaques. *J Clin Invest*. 2011;121(11):4433–4445.
40. DiNapoli SR, Hirsch VM, Brenchley JM. Macrophages in progressive human immunodeficiency virus/simian immunodeficiency virus infections. *J Virol*. 2016;90(17):7596–7606.
41. Williams KC, et al. Perivascular macrophages are the primary cell type productively infected by simian immunodeficiency virus in the brains of macaques: implications for the neuropathogenesis of AIDS. *J Exp Med*. 2001;193(8):905–915.
42. Ho YC, et al. Replication-competent noninduced proviruses in the latent reservoir increase barrier to HIV-1 cure. *Cell*. 2013;155(3):540–551.
43. Calantone N, et al. Tissue myeloid cells in SIV-infected primates acquire viral DNA through phagocytosis of infected T cells. *Immunity*. 2014;41(3):493–502.
44. Baxter AE, et al. Macrophage infection via selective capture of HIV-1-infected $CD4^+$ T cells. *Cell Host Microbe*. 2014;16(6):711–721.
45. Kong LI, et al. West African HIV-2-related human retrovirus with attenuated cytopathicity. *Science*. 1988;240(4858):1525–1529.
46. Avalos CR, et al. Quantitation of productively infected monocytes and macrophages of simian immunodeficiency virus-infected macaques. *J Virol*. 2016;90(12):5643–5656.
47. Knox KS, et al. Reconstitution of CD4 T cells in bronchoalveolar lavage fluid after initiation of highly active antiretroviral therapy. *J Virol*. 2010;84(18):9010–9018.
48. Douek DC, et al. HIV preferentially infects HIV-specific $CD4^+$ T cells. *Nature*. 2002;417(6884):95–98.
49. Micci L, et al. CD4 depletion in SIV-infected macaques results in macrophage and microglia infection with rapid turnover of infected cells. *PLoS Pathog*. 2014;10(10):e1004467.
50. Musich T, et al. A conserved determinant in the V1 loop of HIV-1 modulates the V3 loop to prime low CD4 use and macrophage infection. *J Virol*. 2011;85(5):2397–2405.
51. Swanstrom AE, et al. Derivation and characterization of a CD4-independent, non-CD4-tropic simian immunodeficiency virus. *J Virol*. 2016;90(10):4966–4980.
52. Mefford ME, Kunstman K, Wolinsky SM, Gabuzda D. Bioinformatic analysis of neurotropic HIV envelope sequences identifies polymorphisms in the gp120 bridging sheet that increase macrophage-tropism through enhanced interactions with CCR5. *Virology*. 2015;481:210–222.
53. Dunfee RL, Thomas ER, Wang J, Kunstman K, Wolinsky SM, Gabuzda D. Loss of the N-linked glycosylation site at position 386 in the HIV envelope V4 region enhances macrophage tropism and is associated with dementia. *Virology*. 2007;367(1):222–234.
54. Dunfee RL, et al. The HIV Env variant N283 enhances macrophage tropism and is associated with brain infection and dementia. *Proc Natl Acad Sci USA*. 2006;103(41):15160–15165.
55. Yen PJ, Mefford ME, Hoxie JA, Williams KC, Desrosiers RC, Gabuzda D. Identification and characterization of a macrophage-tropic SIV envelope glycoprotein variant in blood from early infection in SIVmac251-infected macaques. *Virology*. 2014;458–459:53–68.
56. Yen PJ, et al. Loss of a conserved N-linked glycosylation site in the simian immunodeficiency virus envelope glycoprotein V2 region enhances macrophage tropism by increasing CD4-independent cell-to-cell transmission. *J Virol*. 2014;88(9):5014–5028.
57. Tan J, Sattentau QJ. The HIV-1-containing macrophage compartment: a perfect cellular niche? *Trends Microbiol*. 2013;21(8):405–412.
58. McIlroy D, et al. Low infection frequency of macrophages in the spleens of HIV^+ patients. *Res Virol*. 1996;147(2–3):115–121.

59. Hlavacek WS, Stilianakis NI, Notermans DW, Danner SA, Perelson AS. Influence of follicular dendritic cells on decay of HIV during antiretroviral therapy. *Proc Natl Acad Sci USA*. 2000;97(20):10966–10971.
60. Deleage C, et al. Defining HIV and SIV reservoirs in lymphoid tissues. *Pathog Immun*. 2016;1(1):68–106.
61. Heesters BA, et al. Follicular dendritic cells retain infectious HIV in cycling endosomes. *PLoS Pathog*. 2015;11(12):e1005285.
62. Louveau A, et al. Structural and functional features of central nervous system lymphatic vessels. *Nature*. 2015;523(7560):337–341.
63. Ren W, et al. Generation of lineage-related, mucosally transmissible subtype C R5 simian-human immunodeficiency viruses capable of AIDS development, induction of neurological disease, and coreceptor switching in rhesus macaques. *J Virol*. 2013;87(11):6137–6149.
64. Klatt NR, et al. Loss of mucosal $CD103^+$ DCs and $IL\text{-}17^+$ and $IL\text{-}22^+$ lymphocytes is associated with mucosal damage in SIV infection. *Mucosal Immunol*. 2012;5(6):646–657.
65. Harris LD, et al. Mechanisms underlying γδ T-cell subset perturbations in SIV-infected Asian rhesus macaques. *Blood*. 2010;116(20):4148–4157.
66. Price DA, et al. T cell receptor recognition motifs govern immune escape patterns in acute SIV infection. *Immunity*. 2004;21(6):793–803.
67. Keele BF, et al. Identification and characterization of transmitted and early founder virus envelopes in primary HIV-1 infection. *Proc Natl Acad Sci USA*. 2008;105(21):7552–7557.
68. Mattapallil JJ, Douek DC, Hill B, Nishimura Y, Martin M, Roederer M. Massive infection and loss of memory $CD4^+$ T cells in multiple tissues during acute SIV infection. *Nature*. 2005;434(7037):1093–1097.
69. Yao R, Schneider E. Detection of B- and T-cell-specific gene rearrangements in 13 cell lines and 50 clinical specimens using the BIOMED-2 and the original InVivoScribe primers. *Leuk Lymphoma*. 2007;48(4):837–840.
70. Cline AN, Bess JW, Piatak M, Lifson JD. Highly sensitive SIV plasma viral load assay: practical considerations, realistic performance expectations, and application to reverse engineering of vaccines for AIDS. *J Med Primatol*. 2005;34(5–6):303–312.
71. Huelsenbeck JP, Ronquist F. MRBAYES: Bayesian inference of phylogenetic trees. *Bioinformatics*. 2001;17(8):754–755.